STUDIES ON AZULENE-RHODANINE DERIVATIVES COMPLEXATION WITH Pb(II) BY UV-Vis

Cornelia Elena MUȘINĂ (BORȘARU)[1], Ovidiu-Teodor MATICA[2], Eleonora-Mihaela UNGUREANU[3]*

This paper is devoted to the optical characterization of two related azulene-rhodanines and their interaction with Pb(II) ions in acetonitrile solution. The investigations were performed by UV-Vis. The main wavelengths for each compound were established, assessed, and compared with those for the unsubstituted azulene-rhodanine. This comparison confirms that grafting inductive electron-repelling substituents with different volumes and effects on azulene leads to specific optical and complexing properties in relation to Pb(II) ions.

Keywords: UV-Vis, 2-thioxo-thiazolidin-4-ones, azulene, Pb(II) homogeneous complexation, stoichiometry

1. Introduction

Azulene ($C_{10}H_{10}$) is an isomeric hydrocarbon of naphthalene ($C_{10}H_{10}$), with a much more polarized structure than naphthalene, being formed by the fusion of a ring of 7 carbon atoms with a ring of 5 carbon atoms [1, 2]. This less symmetric structure makes azulene exhibit lower ionization energy than naphthalene (symmetrical aromatic compound) and results in higher electron mobility in the molecule and a high dipole moment: $D_{azulene}^{exp} = 1.08$ D [3] > $D_{nafphtalene}^{exp} = 0$ D [4]. Grafting onto azulene of substituents such as methyl and i-propyl, with different volumes and inductive electron-repelling effects, modifies the complexing properties of azulenes. Azulenes can be used as molecular building blocks, useful for various applications, such as molecular recognition of metal ions [5,6]. These modifications in the complexing power of azulenes can be exploited in applications related to molecular recognition in solution or with the help of modified electrodes.

Rhodanine ring is known for its complexing properties towards heavy metals [7]. Rhodanine derivatives are used also in the medical field, as

[1] Ph.D. student, Dept. of Inorganic Chemistry, Physical Chemistry and Electrochemistry, National University of Science and Technology POLITEHNICA Bucharest, Romania, e-mail: borsaru_cornelia@yahoo.com

[2] Ph.D. student, Dept. of Inorganic Chemistry, Physical Chemistry and Electrochemistry, National University of Science and Technology POLITEHNICA Bucharest, Romania, e-mail: maticaovidiu@yahoo.co.uk

[3]*Emeritus Professor, Dept. of Inorganic Chemistry, Physical Chemistry and Electrochemistry, National University of Science and Technology POLITEHNICA Bucharest, e-mail: em_ungureanu2000@yahoo.com

antimicrobial [8, 9], antiviral [10], anti-cancer [10,11], antibacterial [12,13], pan-assay interference compounds (PAINS) [14, 15] or with anti-diabetic activity [16], in the detection of Alzheimer's markers [17], and they are materials with applications in biomedicine [18]. New materials have been developed with applications in the production of supercapacitors [19], and for the protection of various surfaces [20-22] and for the manufacture of photovoltaic cells [23, 24].

In this work several optical properties are studied for two rhodanine-linked azulene structures having different alkyl groups (methyl = Me, i-propyl = i-Pr) as substituents and binding positions on the two azulene rings: 5-(5-isopropyl-3,8-dimethyl-azulen-1-ylmethylene)-2-thioxo-thiazolidin-4-one (**T1**) and 2-thioxo-5-(4,6,8-trimethyl-azulen-1-ylmethylene)-thiazolidin-4-one (**T2**). They were compared with the unsubstituted compound, (Z)-5-(azulen-1-ylmethylene)-2-thioxo-thiazolidin-4-one (**T3**) previously studied [25]. Their proprieties, such as dipole moment (in D), were calculated by DFT methods, which varied in the order **T1**>**T2**>**T3** (9.04>8.84>7.83, respectively, using the B3LYP functional) [7].

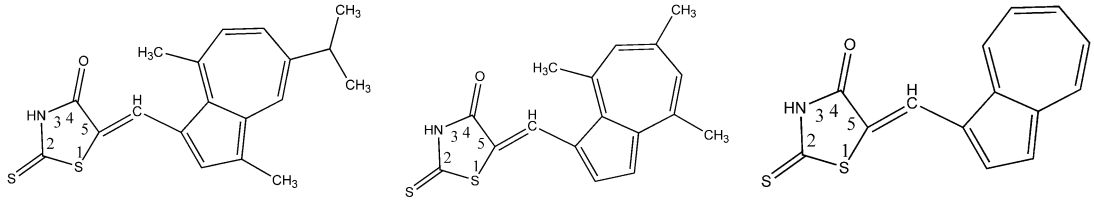

T1 **T2** **T3**

Fig. 1. Structures of the investigated compounds

Electrochemical studies of these compounds have shown that they can lead to modified electrodes with complexing properties towards the investigated heavy metal ions: Cd(II), Pb(II), Cu(II), Hg(II) [26, 27]. Among these ions, the strongest variations in the properties of the modified electrodes occur in the presence of Pb(II) [26, 27]. This different behaviour upon heterogeneous complexation of the films based on **T1** and **T2** ligands can be correlated with the effect of homogeneous complexation of these structures towards Pb(II) ions which was studied in this work.

2. Experimental

The ligands were synthesized according to previously published methods [28]. The UV-Vis studies were performed in acetonitrile HPLC grade from Fluka. Lead (II) nitrate $Pb(NO_3)_2 \bullet H_2O$ from Fluka (Munich, Germany, ≥99.5 %) was used as the source for Pb (II) ions.

The UV-Vis studies were performed on a JASCO V-670 spectrometer in 1 cm optical path quartz cuvettes in freshly dried acetonitrile.

For the study of each ligand (R), the spectra of different concentrations of each ligand in acetonitrile were recorded vs. acetonitrile (ACN). For the study of complexation Pb(II) ions were added as aliquots from stock solutions of $Pb(NO_3)_2$ in demineralized water in the cuvette containing the ligand solved in acetonitrile under stirring. The spectra recorded after 5, 10, 15 minutes were found to be stable, and the spectra after 5 minutes were finally kept and compared.

The complexation reaction shows the formation of a complex consisting of Me metal atoms surrounded by R ligand molecules:

$$mMe + rR = Me_mR_r$$

Tree ways were used to determine the r/m complexation ratio of the Me_mR_r type complex to evaluate the influence of Pb(II) ions on each ligand in solution.

The first way tasted for determination the r/m complexation ratio is the molar ratio method [29, 30], which consists in the graphical representation of the maximum intensity peak absorbance, for a specific wavelength, as a function of [Pb(II)] / [R], and observing the change in the slope. The value of the ratio at the point where the slope of the line changes is equal to the ratio r/m.

The second way for determination the r/m complexation ratio is the method of continuous variations (Job) [29,30], and consisted in measuring the absorbance, for a specific wavelength, of a series of solutions, in which the molar fraction (X = [Me]/([Me] + [R]) of the metal varied between 0 and 1. The molar fraction (X) at which there is a minimum or maximum absorbance is related to the stoichiometric ratio in the complex, through the relationship: r/m= (1 - X)/X. If the dissociation of the complex is significant then the minimum or maximum absorbance points were determined by extrapolating the linear domains.

The third way for determination the r/m complexation ratio was the Mollard method [29, 31] concerned in measuring the absorbance for two solutions, one containing the metal ion in concentration C_M and the ligand in large excess, for which the absorbance is A_M, and one in which the metal ion is in excess *vs.* the ligand concentration C_R for which the absorbance is A_R. The value of r/m was given by the relationship (1)

$$r/m = C_M A_R/ (C_R A_M) \quad (1)$$

3. Results and Discussion

a. UV-Vis studies for ligands

Figs. 2 and 3 show the spectra obtained for different concentrations of ligand **T1** and **T2**, respectively in ACN. The maxima were examined as wavelengths and absorbance. The absorbance was plotted *vs.* each ligand concentration, and their linear dependences were examined (Table 1, Table 2, respectively). For **T1** and **T2** in ACN, 4 main peaks were identified for which calibration lines of the type A = a + b·c were determined, where A = absorbance at the specific wavelength, a =

ordinate at the origin, b = slope of the line, and c = the ligand concentration in the tank (Table 1, respectively Table 2). The coordinates of the peaks were compared with those of the unsubstituted compound **T3**, obtained from the UV-Vis spectra of the solutions in ACN recorded under the same conditions. The spectra obtained in ACN for compounds **T1**-**T3** were compared with those reported in methanol [28].

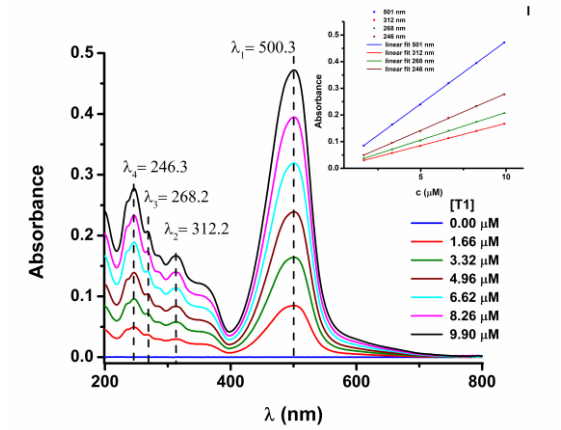

Fig. 2. UV-Vis spectra for different concentrations of **T1** and dependence of absorbances on **T1** concentration (inset)

Table 1

Linear dependence of absorbance (A) *vs.* concentration (c), extinction coefficient (ε) for T1 peaks at specific maximum wavelength in ACN (λ), and extinction coefficient (ε') for peaks at specific maximum wavelength in methanol [28]

λ (nm)	Equation	Pearson's r	ε ($M^{-1}cm^{-1}$)	log(ε)	λ' (nm)	log(ε')
500	$A_{\lambda 1} = 0.0071 + 0.04696 \cdot c$	0.9999	46960	4.672	502	4.64
312	$A_{\lambda 2} = 0.0018 + 0.0167 \cdot c$	0.9997	16700	4.223	307	4.16
268	$A_{\lambda 4} = 0.0025 + 0.0207 \cdot c$	0.9997	20720	4.316	268	4.26
246	$A_{\lambda 5} = 0.0032 + 0.0278 \cdot c$	0.9997	27800	4.444	247	4.41

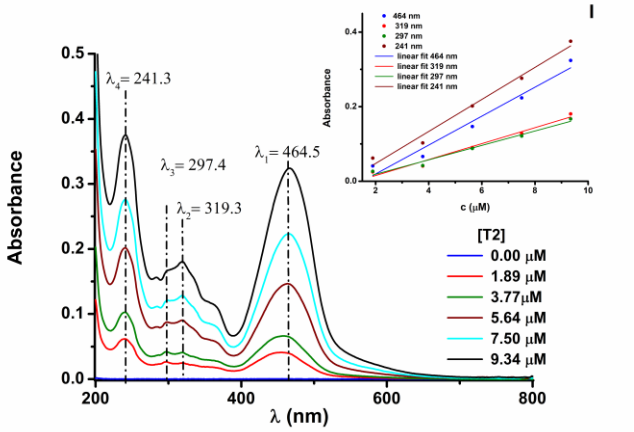

Fig. 3. UV-Vis spectra for different concentrations of **T2** and dependence of absorbances on **T2** concentration (inset)

Table 2

Linear dependence of absorbance (A) *vs.* concentration (c), extinction coefficient (ε) for T2 peaks at specific maximum wavelength in ACN (λ), and extinction coefficient (ε') for peaks at specific maximum wavelength in methanol (λ') [28]

λ (nm)	Equation	Pearson's r	ε ($M^{-1}cm^{-1}$)	log(ε)	λ' (nm)	log(ε')
465	$A_{\lambda 1} = -0.0582 + 0.03879 \cdot c$	0.9831	38790	4.59	477	4.53
319	$A_{\lambda 2} = -0.02756 + 0.0214 \cdot c$	0.9879	21400	4.33	325	4.11
297	$A_{\lambda 3} = -0.01997 + 0.01934 \cdot c$	0.9894	19340	4.29	305	4.09
241	$A_{\lambda 4} = -0.03833 + 0.04296 \cdot c$	0.9921	42960	4.63	251	4.33

From Table 2 and Table 3 linear dependency of absorbance on **T1**, and **T2** ligand concentration, respectively, of the main peaks was noticed, as in case of unsubstituted ligand **T3** (Table 3).

Table 3

Linear dependence of absorbance (A) *vs.* concentration (c), extinction coefficient (ε) for T3 peaks at specific maximum wavelength in ACN (λ) [25], **and extinction coefficient (ε′) for peaks at specific maximum wavelength in methanol (λ')** [28]

λ (nm)	Equation	Pearson's r	ε ($M^{-1}cm^{-1}$)	log(ε)	λ' (nm)	log(ε')
456	$A_{\lambda 1} = 0.0145 + 0.0296 \cdot c$	0.9992	29620	4.47	468	4.47
435	$A_{\lambda 2} = 0.0318 + 0.0295 \cdot c$	0.9953	29470	4.47	-	-
333	$A_{\lambda 3} = 0.011 + 0.0093 \cdot c$	0.9903	9290	3.97	338	3.82
288	$A_{\lambda 4} = 0.0253 + 0.0169 \cdot c$	0.9871	16880	4.23	293	3.95
226	$A_{\lambda 5} = 0.0188 + 0.0164 \cdot c$	0.9848	16420	4.22	228	4.07

Comparison between ligand spectra

The absorption bands at longer wavelengths for the **T1**, **T2**, and **T3** derivatives can be associated with a localized π → π* transition throughout the molecular system. These transitions occur at the wavelengths located in the order: **T1**>**T2**>**T3**, which correspond in transitions energies in the reverse order: **T3**>**T2**>**T1**. The results agree with other spectral data [32].

Table 4 resumes the main spectral to data for **T1**-**T3** corresponding to the 4 peaks identified in the spectra, when scanning from higher to lower wavelengths.

In ACN solvent the compounds **T1**-**T3** present specific absorption maxima for transitions observed at wavelengths that vary depending on the structure of the ligands. For instance, for these ligands the transition from visible occurs, respectively, at λmax: 500>465>456, and the corresponding absorbances decrease in the same order: **T1**>**T2**>**T3**. Consequently, the molar extinction coefficients have the same trend. They present close values in the two tested solvents, ACN and methanol (Table 4).

In methanol, compounds **T1**-**T3** show absorption maxima at longer wavelengths than in ACN, as it results from the comparison of the values from Column 4 with those from Column 1. The molar extinction coefficients in methanol are slightly lower than those obtained in ACN, as it results from the comparison of the values from Column 5 and those from Column 3 of Table 4.

Table 4

Extinction coefficients (ε, ε') at specific maximum wavelengths (λ, λ') for T1, T2 and T3 in two solvents, ACN (ε, λ) and methanol (λ', ε') [28], respectively

Ligand	λ (nm)	ε ($M^{-1}cm^{-1}$)	log(ε)	λ' (nm)	log(ε')
	1	2	3	4	5
T1	500 (peak 1)	46960	4.672	502	4.64
T2	465 (peak 1)	38790	4.589	477	4.53
T3	456 (peak 1)	29620	4.472	468	4.47
T1	312 (peak 2)	16700	4.223	307	4.16
T2	319 (peak 2)	21400	4.33	325	4.11
T3	333 (peak 2)	9290	3.968	338	3.82
T1	268 (peak 3)	20720	4.316	268	4.26
T2	297 (peak 3)	19340	4.286	305	4.09
T3	288 (peak 3)	16880	4.227	293	3.95
T1	246 (peak 4)	27800	4.444	247	4.41
T2	241 (peak 4)	42960	4.633	251	4.33
T3	226 (peak 4)	16420	4.215	228	4.07

b. UV-Vis studies for ligands complexation with Pb(II)

The spectra evolutions were examined as absorbance and wavelengths in respect to the ratio between Pb(II) concentration and ligand concentration ([Pb(II)]/[**R**]), or molar fraction of Pb(II) in solution ([Pb(II)]/([**R**] + [Pb(II)])), according to all methods for each ligand, as seen for **T1** in Fig. 4. Fig. 5, and Table 5; for **T2** in Fig. 6. Fig. 7, and Table 6.

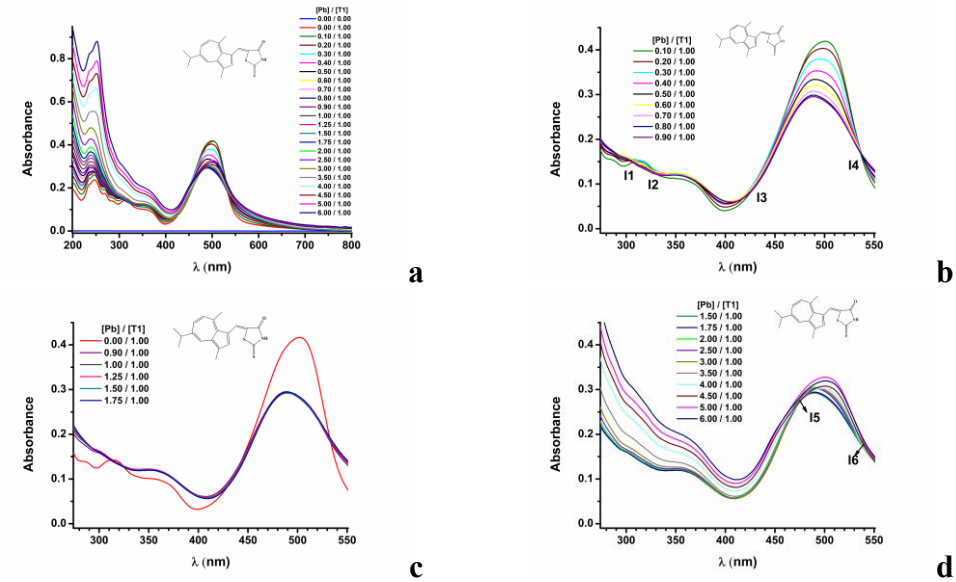

Fig 4. UV-Vis spectra for [**T1**] = 8.75 μM in solutions for different [Pb (II)] / [**T1**] ratios between: 0-6 (**a**), 0.1- 0.9 (**b**); 0.9- 1.75 (**c**) and 1.5- 6 (**d**)

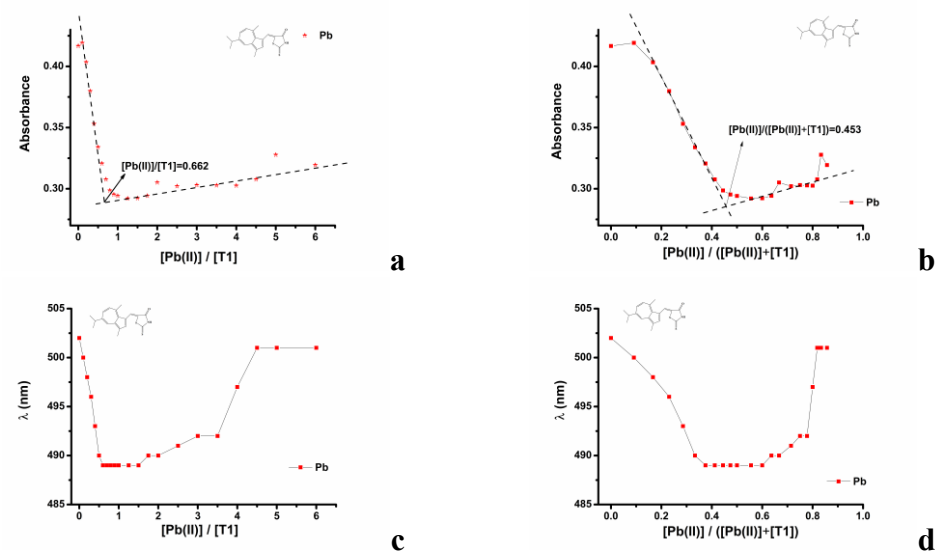

Fig 5. Variations of absorbance (**a**, **b**) and wavelength (**c**, **d**) with [Pb(II)]/[**T1**] ratio (**a**, **c**) and with [Pb(II)]/([Pb(II)]+[**T1**]) ratio (**b**, **d**)

Table 5

Ratios r/m for $(Pb)_m(T1)_r$ according to Mollard method for absorbance (A)

Crt. No.	Excess of Pb			Excess of Ligand			r/m	m	r	Complex formula
	[Pb]/[**T1**]	[**T1**] µM	A	[Pb]/[**T1**]	[Pb] µM	A				
1a	6/1	8.32	0.319	0.2/1	1.76	0.403	5.98	1	5.98	Pb**T1**$_6$
2a	5/1	8.39	0.328	0.2/1	1.76	0.403	5.88	1	5.88	Pb**T1**$_6$
3a	4/1	8.46	0.303	0.2/1	1.76	0.403	6.31	1	6.31	Pb**T1**$_6$
4a	3.5/1	8.50	0.303	0.2/1	1.76	0.403	6.45	1	6.45	Pb**T1**$_6$
5a	3/1	8.53	0.328	0.2/1	1.76	0.403	6.47	1	6.47	Pb**T1**$_6$
1b	6/1	8.32	0.319	0.3/1	2.63	0.380	3.76	1	3.76	Pb**T1**$_4$
2b	5/1	8.39	0.328	0.3/1	2.63	0.380	3.69	1	3.69	Pb**T1**$_4$
3b	4/1	8.46	0.303	0.3/1	2.63	0.380	3.97	1	3.97	Pb**T1**$_4$
4b	3.5/1	8.50	0.303	0.3/1	2.63	0.380	4.05	1	4.05	Pb**T1**$_4$
5b	3/1	8.53	0.323	0.3/1	2.63	0.380	4.06	1	4.06	Pb**T1**$_4$
1c	6/1	8.32	0.319	0.4/1	3.51	0.353	2.62	1	2.62	Pb**T1**$_3$
2c	5/1	8.39	0.328	0.4/1	3.51	0.353	2.58	1	2.58	Pb**T1**$_3$
3c	4/1	8.46	0.303	0.4/1	3.51	0.353	2.77	1	2.77	Pb**T1**$_3$
4c	3.5/1	8.50	0.303	0.4/1	3.51	0.353	2.83	1	2.83	Pb**T1**$_3$
5c	3/1	8.53	0.323	0.4/1	3.51	0.353	2.84	1	2.84	Pb**T1**$_3$
1d	6/1	8.32	0.319	0.5/1	4.38	0.334	1.99	1	1.99	Pb**T1**$_2$
2d	5/1	8.39	0.328	0.5/1	4.38	0.334	1.95	1	1.95	Pb**T1**$_2$
3d	4/1	8.46	0.303	0.5/1	4.38	0.334	2.10	1	2.10	Pb**T1**$_2$
4d	3.5/1	8.50	0.303	0.5/1	4.38	0.334	2.14	1	2.14	Pb**T1**$_2$
5d	3/1	8.53	0.323	0.5/1	4.38	0.334	2.15	1	2.15	Pb**T1**$_2$
1e	6/1	8.32	0.319	0.6/1	5.25	0.321	1.59	1	1.59	Pb_2**T1**$_3$
2e	5/1	8.39	0.328	0.6/1	5.25	0.321	1.56	1	1.56	Pb_2**T1**$_3$
3e	4/1	8.46	0.303	0.6/1	5.25	0.321	1.68	1	1.68	Pb_2**T1**$_3$
4e	3.5/1	8.50	0.303	0.6/1	5.25	0.321	1.71	1	1.71	Pb_2**T1**$_3$
5e	3/1	8.53	0.323	0.6/1	5.25	0.321	1.72	1	1.72	Pb_2**T1**$_3$

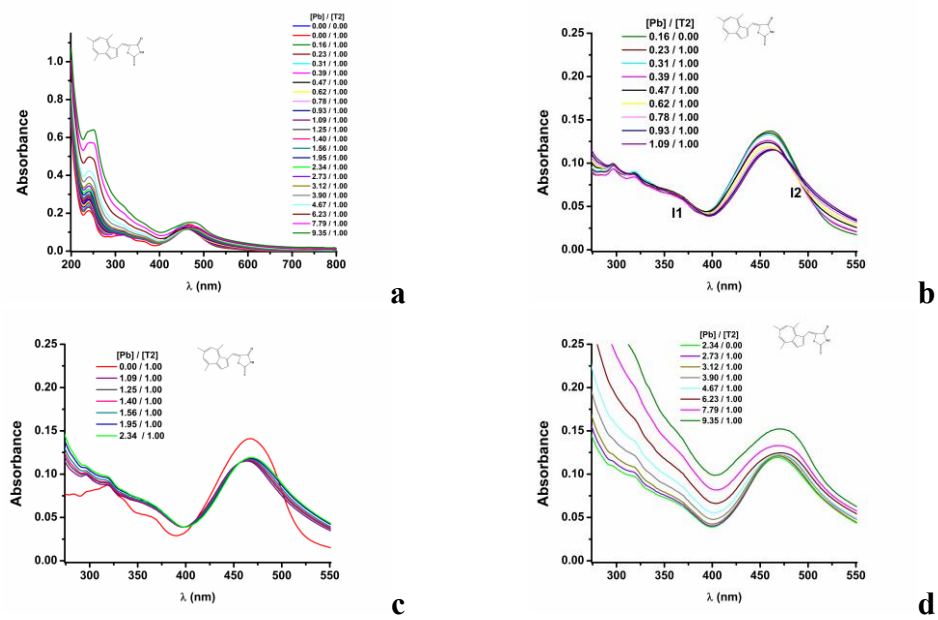

Fig 6. UV-Vis spectra for [**T2**] = 5.13 μM in solutions for different [Pb (II)] / [**T2**] ratios between: 0-9.35 (**a**), 0.16-1.09 (**b**), 1.09- 2.34(**c**), and 2.34- 9.35 (**d**).

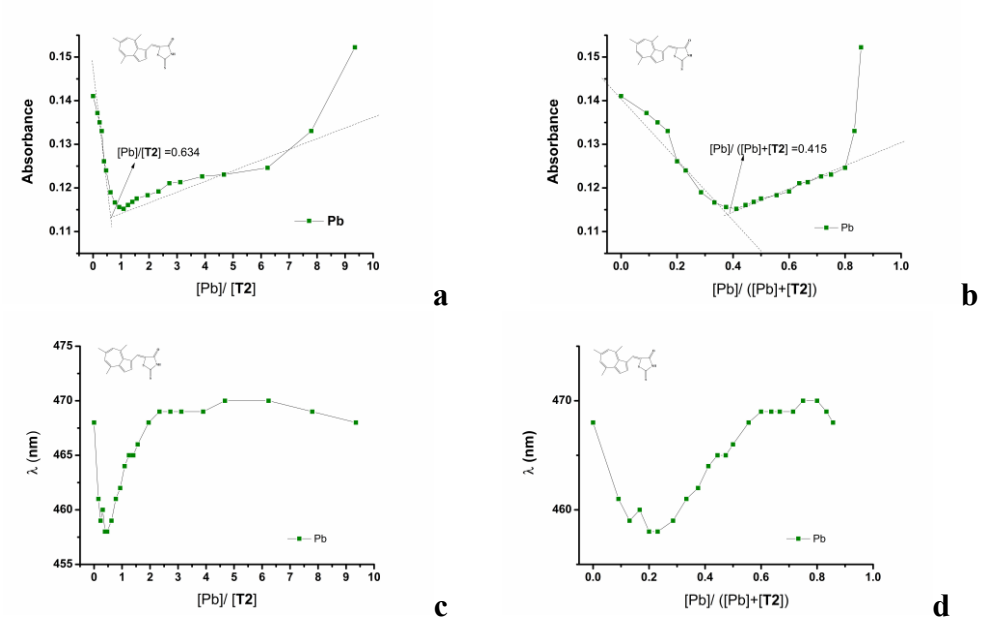

Fig 7. Variations of absorbance (**a**, **b**) and wavelength (**c**, **d**) with [Pb(II)]/[**T2**] ratio (**a**, **c**) and with [Pb(II)]/([Pb(II)]+[**T2**]) ratio (**b**, **d**)

Figs. 4, 5, 6, and 7 were compared with Fig. 8, which contains the representations of the absorbance (a, b) and the wavelength of the absorption peak in the visible domain (c, d) in relation to the molar ratio [metal]/]ligand] (a, c,

respectively) or in relation to the molar fraction of the metal in solution (b, d, respectively) for the complexation of unsubstituted azulene ligand **T3**. From the examination of all the curves in Figs. 6a, 7a, 8a it is difficult to follow the effect of complexation. However, the examination of absorbance variations over narrow ranges of molar ratios [Pb(II)]/[ligand] helps the determination of m/r complexation ratios.

Table 6

Ratios r/m for $(Pb)_m(T2)_r$ according to Mollard method

Crt. No.	Excess of Pb			Excess of Ligand			r/m	m	r	Complex formula
	[Pb]/[**T2**]	[**T2**] µM	A	[Pb]/[**T2**]	[Pb] µM	A				
1a	9.35/1	4.88	0.152	0.23/1	1.26	0.135	3.43	1	3.43	Pb_2**T2**$_7$
2a	7.79/1	4.92	0.133	0.23/1	1.26	0.135	3.96	1	3.96	Pb**T2**$_4$
3a	4.67/1	5.01	0.123	0.23/1	1.26	0.135	4.29	1	4.29	Pb**T2**$_4$
4a	3.9/1	5.03	0.123	0.23/1	1.26	0.135	4.36	1	4.36	Pb**T2**$_4$
5a	3.12/1	5.05	0.121	0.23/1	1.26	0.135	4.4	1	4.4	Pb**T2**$_4$
1b	9.35/1	4.88	0.152	0.31/1	1.68	0.133	2.54	1	2.54	Pb_2**T2**$_5$
2b	7.79/1	4.92	0.133	0.31/1	1.68	0.133	2.92	1	2.92	Pb**T2**$_3$
3b	4.67/1	5.01	0.123	0.31/1	1.68	0.133	3.17	1	3.17	Pb**T2**$_3$
4b	3.9/1	5.03	0.123	0.31/1	1.68	0.133	3.22	1	3.22	Pb**T2**$_3$
5b	3.12/1	5.05	0.121	0.31/1	1.68	0.133	3.25	1	3.25	Pb**T2**$_3$
1c	9.35/1	4.88	0.152	0.39/1	2.10	0.126	1.92	1	1.92	Pb**T2**$_2$
2c	7.79/1	4.92	0.133	0.39/1	2.10	0.126	2.22	1	2.22	Pb**T2**$_2$
3c	4.67/1	5.01	0.123	0.39/1	2.10	0.126	2.41	1	2.41	Pb_2**T2**$_5$
4c	3.9/1	5.03	0.123	0.39/1	2.10	0.126	2.45	1	2.45	Pb_2**T2**$_5$
5c	3.12/1	5.05	0.121	0.39/1	2.10	0.126	2.47	1	2.47	Pb_2**T2**$_5$
1d	9.35/1	4.88	0.152	0.47/1	2.52	0.124	1.58	1	1.58	Pb_2**T2**$_3$
2d	7.79/1	4.92	0.133	0.47/1	2.52	0.124	1.82	1	1.82	Pb**T2**$_2$
3d	4.67/1	5.01	0.123	0.47/1	2.52	0.124	1.97	1	1.97	Pb**T2**$_2$
4d	3.9/1	5.03	0.123	0.47/1	2.52	0.124	2.01	1	2.01	Pb**T2**$_2$
5d	3.12/1	5.05	0.121	0.47/1	2.52	0.124	2.02	1	2.02	Pb**T2**$_2$
1e	9.35/1	4.88	0.152	0.62/1	3.36	0.119	1.14	1	1.14	Pb**T2**
2e	7.79/1	4.92	0.133	0.62/1	3.36	0.119	1.31	1	1.31	Pb**T2**
3e	4.67/1	5.01	0.123	0.62/1	3.36	0.119	1.42	1	1.42	Pb_2**T2**$_3$
4e	3.9/1	5.03	0.123	0.62/1	3.36	0.119	1.45	1	1.45	Pb_2**T2**$_3$
5e	3.12/1	5.05	0.121	0.62/1	3.36	0.119	1.46	1	1.46	Pb_2**T2**$_3$

Application of the methods

From the examination of all the curves in Fig. 6a it is difficult to follow the effect of complexation of Pb(II) with **T1**. The examination of absorbance variations over narrow ranges of molar ratios [Pb(II)]/[**T1**] shows that important variations occur over the range of molar ratios 0.15 – 0.9 (Fig. 4b). 4 isosbestic points appeared (I1 - I4). On the range 0.9 -1.75 (Fig. 4c) no important variations are noticed for the solutions, the spectra being clearly different from that of the ligand (represented by the red line). On the range 1.5-6 (Fig. 4d) two isosbestic points can be noticed.

In case of **T2** the examination of absorbance changes over narrow ranges of molar ratios [Pb(II)]/[**T2**] shows that important variations occur over the range of molar ratios 0.16 – 1.09 (Fig. 6b). 2 isosbestic points appeared (I1 - I2). On the range 1.09 - 2.34 (Fig. 6c) no important variations are observed for the solutions, the spectrum being clearly different from that of the ligand (represented by the red line). On the range 2.34 - 9.35 (Fig. 6d) no isosbestic point can be noticed. Only variations of absorbances are noticed due to the increase in the amount of water in the solution together with the amount of Pb(II) ions introduced to reach the ratios of [Pb(II)]/[**T2**] studied.

In case of **T3** the examination of absorbance changes over narrow ranges of molar ratios [Pb(II)]/[**T3**] shows that important variations occur over the range of molar ratios 0 – 1.26 (Fig. 8b). 4 isosbestic points appeared (I1 -I4). On the range 0.9 -1,76 (Fig. 8c) no important variations are noticed for the solutions, the spectrum being clearly different from that of the ligand (represented by the blue line). On the range 1.6-5 (Fig. 8d) one isosbestic point can be estimated. Only variations of the absorbances due to the increase in the amount of water in the solution together with the amount of Pb(II) ions introduced to reach the ratios of [Pb(II)]/[**T3**] are noticed.

Molar ratio method

Figs. 5a, 5c, 7a,7c, 9a, 9c show the formation of several complexes with different stoichiometries and stabilities. At low amounts of Pb, complexes are formed with **T1**, evidenced by the absorbance inflection peaks located at 0.662 with A = 0.295 (for **T1**), 0.634 with A = 0.112 (for **T2**) and 0.735 with A = 0.3 (for **T3**). Also, the variation of the wavelength with increasing amounts of Pb (Figs. 5c, 7c, 9c) is noticed.

Method of continuous variations (Job)

Figs. 5b, 7b, 9b highlight the formation of several complexes with different stoichiometries for **T1**, **T2** and **T3**, evidenced by the inflection points of the absorbances at 0.453 (for **T1**), 0.415 (for **T2**) and 0.589 (for **T3** [25]). The variation of wavelengths with the mole fraction of Pb in solution was also recorded showing several inflexions confirming the formation of different complexes. The first inflection occurs for **T1** at 489 nm (absorbance of 0.295, Fig. 5d), and for **T2** at 458 nm (absorbance of 0.112, Fig. 7d), while for **T3** it is at 455 nm (absorbance of 0.3 [25], Fig. 9d).

Mollard method

Tables 5, 6 and 7 indicate the stoichiometry of the complexes formed in solutions with increasing amounts of Pb. A complex with stoichiometry 1/6 is initially formed for **T1**, then it changes to 1/4, 1/3, 1/2 and finally 2/3.

For **T2** a complex with stoichiometry 1/4 is initially formed for **T1**, then it changes to 1/3, 2/5, 1/2 and finally 2/3.

For **T3** a complex with stoichiometry 1/5 is initially formed for **T1**, than it changes to 1/3, 2/5, 1/2 and finally 2/3.

For **T3** the wavelength varies continuously for molar ratios between 0 and 1.5, then it is constant for molar ratio values between 1.5 and 2.5 corresponding to a Pb_2(**T3**)$_3$ complex, then increases continuously.

The most stable complexes with Pb(II) are those formed by **T2**, since the wavelength is practically constant for [Pb(II)]/[**T2**] molar ratios range between 2.5 and 10.

The electron-repulsive groups on the azulene nuclei in **T1** and **T2** that increase the complexing strength of the rhodanine ring make these ligands better complex the Pb(II) ion in solution than the unsubstituted ligand **T3**. Among them, the best complexing ligand appears to be **T2**.

Table 7

Ratios r/m for (Pb)$_m$(T3)$_r$ according to Mollard method for absorbance (A)

Crt. No.	Excess of Pb			Excess of Ligand			r/m	m	r	Complex formula
	[Pb]/[**T3**]	[**T3**] µM	A	[Pb]/[**T3**]	[Pb] µM	A				
1a	5/1	12.07	0.398	0.2/1	2.62	0.380	4.39	1	4.39	(Pb)(**T3**)$_4$
2a	4.5/1	12.14	0.388	0.2/1	2.62	0.380	4.53	1	4.53	(Pb)$_2$(**T3**)$_9$
3a	4/1	12.22	0.376	0.2/1	2.62	0.380	4.71	1	4.71	(Pb)$_2$(**T3**)$_9$
4a	3.5/1	12.29	0.369	0.2/1	2.62	0.380	4.82	1	4.82	(Pb)(**T3**)$_5$
5a	3/1	12.37	0.348	0.2/1	2.62	0.380	5.15	1	5.15	(Pb)(**T3**)$_5$
1b	5/1	12.07	0.398	0.3/1	3.93	0.367	2.82	1	2.82	(Pb)(**T3**)$_3$
2b	4.5/1	12.14	0.388	0.3/1	3.93	0.367	2.92	1	2.92	(Pb)(**T3**)$_3$
3b	4/1	12.22	0.376	0.3/1	3.93	0.367	3.04	1	3.04	(Pb)(**T3**)$_3$
4b	3.5/1	12.29	0.369	0.3/1	3.93	0.367	3.11	1	3.11	(Pb)(**T3**)$_3$
5b	3/1	12.37	0.348	0.3/1	3.93	0.367	3.33	1	3.33	(Pb)(**T3**)$_3$
1c	5/1	12.07	0.398	0.4/1	5.23	0.352	2.04	1	2.04	(Pb)(**T3**)$_2$
2c	4.5/1	12.14	0.388	0.4/1	5.23	0.352	2.11	1	2.11	(Pb)(**T3**)$_2$
3c	4/1	12.22	0.376	0.4/1	5.23	0.352	2.19	1	2.19	(Pb)(**T3**)$_2$
4c	3.5/1	12.29	0.369	0.4/1	5.23	0.352	2.24	1	2.24	(Pb)(**T3**)$_2$
5c	3/1	12.37	0.348	0.4/1	5.23	0.352	2.40	1	2.40	(Pb)$_2$(**T3**)$_5$
1d	5/1	12.07	0.398	0.5/1	6.53	0.339	1.58	1	1.58	(Pb)$_2$(**T3**)$_3$
2d	4.5/1	12.14	0.388	0.5/1	6.53	0.339	1.63	1	1.63	(Pb)$_2$(**T3**)$_3$
3d	4/1	12.22	0.376	0.5/1	6.53	0.339	1.69	1	1.69	(Pb)$_2$(**T3**)$_3$
4d	3.5/1	12.29	0.369	0.5/1	6.53	0.339	1.73	1	1.73	(Pb)$_2$(**T3**)$_3$
5d	3/1	12.37	0.348	0.5/1	6.53	0.339	1.85	1	1.85	(Pb)(**T3**)$_2$
1e	5/1	12.07	0.398	0.6/1	7.83	0.336	1.3	1	1.3	(Pb)$_2$(**T3**)
2e	4.5/1	12.14	0.388	0.6/1	7.83	0.336	1.35	1	1.35	(Pb)$_2$(**T3**)
3e	4/1	12.22	0.376	0.6/1	7.83	0.336	1.40	1	1.40	(Pb)$_2$(**T3**)$_3$
4e	3.5/1	12.29	0.369	0.6/1	7.83	0.336	1.43	1	1.43	(Pb)$_2$(**T3**)$_3$
5e	3/1	12.37	0.348	0.6/1	7.83	0.336	1.53	1	1.53	(Pb)$_2$(**T3**)$_3$

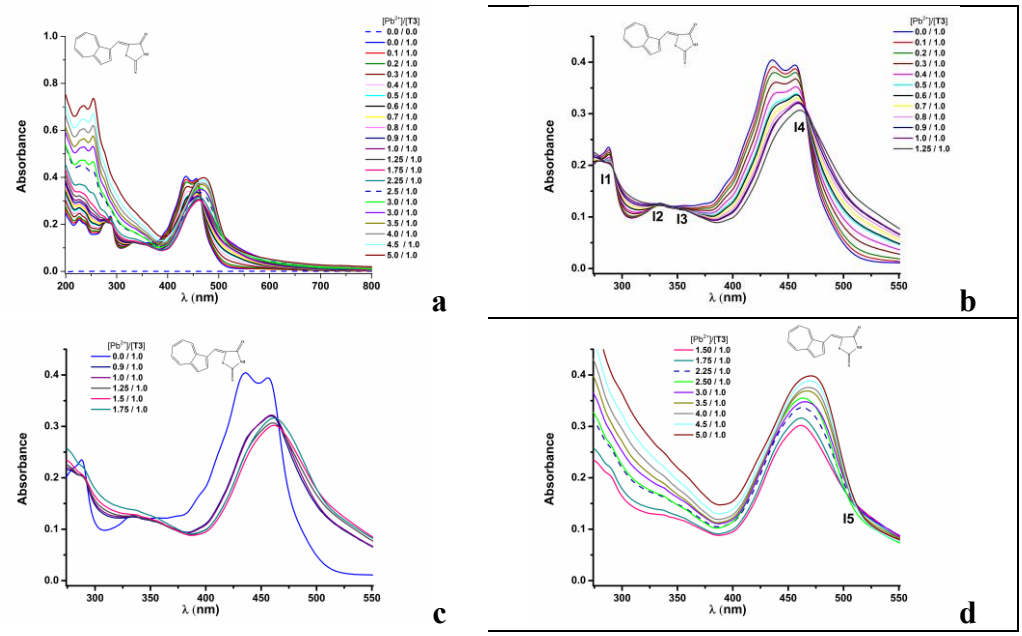

Fig 8. UV-Vis spectra for [**T3**] = 12.8 μM in solutions for different [Pb (II)] / [**T3**] ratios between: 0-5 (**a**), 0-1.25 (**b**); 0.9-1.75 (**c**) and 1.5-5 (**d**)

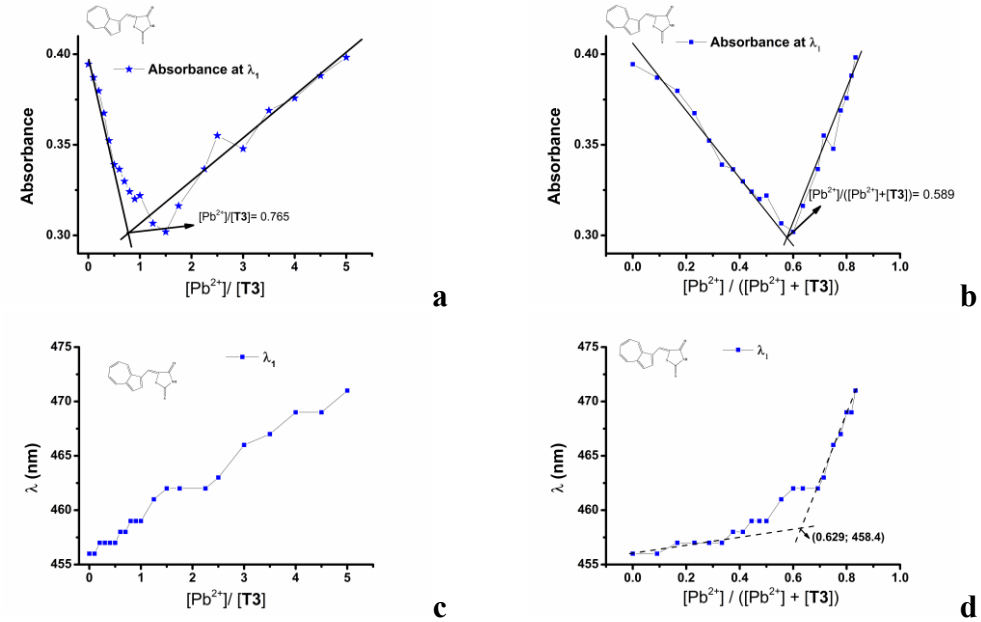

Fig 9. Variations of absorbance (**a**, **b**) and wavelength (**c**, **d**) with [Pb(II)]/[**T3**] ratio (**a**, **c**) and with [Pb(II)]/([Pb(II)]+[**T3**]) ratio (**b**, **d**)

This result is different from the results obtained from the study of Pb(II) complexation using chemically modified electrodes (CMEs) based on **T1-T3**, where the complexation indicated the following order in peak height for Pb(II):

T2~T3>>T1 [33]. The ligand substituted with i-Pr (**T1**) appears unfavorable for the analysis of Pb(II) by the method of heterogeneous recognition on the surface of CMEs. This result confirms that a ligand can act differently in homogeneous or heterogeneous recognition, the order of complexation strength in heterogeneous complexation being affected not only by the structure of the ligand, but also by the structure of the films that form on the surface of the CMEs.

4. Conclusion

This work explored several optical properties of 5-(5-isopropyl-3,8-dimethyl-azulen-1-ylmethylene)-2-thioxo-thiazolidin-4-one (**T1**) and 2-thioxo-5-(4,6,8-trimethyl-azulen-1-ylmethylene)-thiazolidin-4-one (**T2**) in comparison with those of unsubstituted compound, (Z)-5-(azulen-1-ylmethylene)-2-thioxo-thiazolidin-4-one (**T3**), recorded in acetonitrile and methanol. The three compounds exhibit solvatochromism. In methanol, compounds T1-T3 show absorption maxima at longer wavelengths than in acetonitrile, and the molar extinction coefficients are slightly lower than those obtained in acetonitrile. This observation shows that UV-Vis transitions are easier to achieve in methanol and can be useful in applications that can be carried out in different solvents.

The UV-Vis study of their complexation against Pb(II) in acetonitrile solution put in evidence the formation of main soluble complexes for [Pb(II)]/[ligand] molar ratio less the unity, corresponding to the formula $Pb(ligand)_2$, but also the formation of other complexes. The three ligands have also complexed with different stoichiometries $Pb_2(ligand)_3$, $Pb(ligand)_3$, $Pb(ligand)_6$. The stoichiometric ratios in the main complexes were established by three methods with similar results.

The molar ratio method and the method of continuous variations (Job) allowed to highlight the formation of several complexes with different stoichiometries-evidenced by the absorbance inflection peaks and by the variation of the wavelength with increasing Pb amount.

The Mollard method led to the calculation of the stoichiometries of complexes formed during complexation. The most stable complexes appear to be those formed by **T2**, since the wavelength is practically constant for the range of molar ratios [Pb(II)]/[**T2**] between 2.5 and 10.

The electron-withdrawing groups on the azulene core of **T1** and **T2**, which increase the complexing power of the rhodanine ring, make these ligands better complex the Pb(II) ion. The best complexing agent seems to be **T2**.

The obtained results confirm that grafting onto azulene substituents with electron-repelling effects, such as methyl and i-propyl, leads to optical properties that vary with the polar solvent and to specific complexing properties with respect to the Pb(II) ion in solution.

REFERENCES

[1] *A.C. Răzuș*, Azulene moiety as electron reservoir in positively charged systems; a short survey, Symmetry, Vol. Iss. 4, 2020, DOI: https://doi.org/10.3390/sym13040526.

[2] *P. Das*, *S. Ray*, A Brief Review on Different Reactions of Rhodanine ** Funding: This work was supported by the Department of Science and Technology, Ministry of Science and Technology, India and DST SERB-SURE (file number: SUR/2022/004905) grant, Journal of Heterocyclic Chemistry, Vol. **62**, 2025, DOI: https://doi.org/https://doi.org/10.1002/jhet.4924.

[3] *A.G. Jr. Anderson*, *B.M. Steckler*, Azulene. VIII. A Study of the Visible Absorption Spectra and Dipole Moments of Some 1- and 1,3-Substituted Azulenes1,2, Journal of the American Chemical Society, Vol. **81**, Iss. 18, 1959, DOI: https://doi.org/10.1021/ja01527a046.

[4] *V. Librando*, *A. Alparone*, Structure, vibrational properties and polarizabilities of methylnaphthalene isomers. a quantum-mechanical approach, Polycyclic Aromatic Compounds, Vol. **27**, Iss. 1, 2007, DOI: https://doi.org/10.1080/10406630601144770.

[5] *B. Fabre*, Chapter 2 - Conjugated polymer films for molecular and ionic recognition. In H. Singh Nalwa, ed., Handbook of Advanced Electronic and Photonic Materials and Devices (Burlington: Academic Press, 2001), pp. 103–129. https://doi.org/https://doi.org/10.1016/B978-012513745-4/50065-2.

[6] *R. Abhijna Krishna*, *S. Velmathi*, A review on fluorimetric and colorimetric detection of metal ions by chemodosimetric approach 2013–2021, Coordination Chemistry Reviews, Vol. **459**, 2022, DOI: https://doi.org/https://doi.org/10.1016/j.ccr.2021.214401.

[7] *A.-A. Vasile (Corbei)*, *E.-M. Ungureanu*, *G. Stanciu*, *M. Cristea*, *A. Stefaniu*, Evaluation of (Z)-5-(Azulen-1-ylmethylene)-2-thioxothiazolidin-4-ones Properties Using Quantum Mechanical Calculations, Symmetry, Vol. **13**, Iss. 8, 2021DOI: https://doi.org/10.3390/sym13081462.

[8] *M. Krátký*, *J. Vinšová*, *J. Stolaříková*, Antimicrobial activity of rhodanine-3-acetic acid derivatives, Bioorganic & Medicinal Chemistry, Vol. **25**, Iss. 6, 2017, DOI: https://doi.org/https://doi.org/10.1016/j.bmc.2017.01.045.

[9] *N.A. Abdel Hafez*, *M.A. Elsayed*, *M.M. El-Shahawi*, *G.E.A. Awad*, *K.A. Ali*, Synthesis and Antimicrobial Activity of New Thiazolidine-Based Heterocycles as Rhodanine Analogues, Journal of Heterocyclic Chemistry, Vol. **55**, Iss. 3, 2018, DOI: https://doi.org/https://doi.org/10.1002/jhet.3087.

[10] *S.M. Mousavi*, *M. Zarei*, *S.A. Hashemi*, *A. Babapoor*, *A.M. Amani*, A conceptual review of rhodanine: current applications of antiviral drugs, anticancer and antimicrobial activities, Artificial Cells, Nanomedicine, and Biotechnology, Vol. **47**, Iss. 1, 2019 DOI: https://doi.org/10.1080/21691401.2019.1573824.

[11] *H. Sung*, *J. Ferlay*, *R.L. Siegel*, *M. Laversanne*, *I. Soerjomataram*, *A. Jemal*, *F. Bray*, Global Cancer Statistics 2020: GLOBOCAN Estimates of Incidence and Mortality Worldwide for 36 Cancers in 185 Countries, CA: A Cancer Journal for Clinicians, Vol. **71**, Iss. 3, 2021, DOI: https://doi.org/https://doi.org/10.3322/caac.21660.

[12] *Y. Wu*, *X. Ding*, *S. Xu*, *Y. Yang*, *X. Zhang*, *C. Wang*, *H. Lei*, *Y. Zhao*, Design and synthesis of biaryloxazolidinone derivatives containing a rhodanine or thiohydantoin moiety as novel antibacterial agents against Gram-positive bacteria, Bioorganic & Medicinal Chemistry Letters, Vol. **29**, Iss. 3, 2019, DOI: https://doi.org/https://doi.org/10.1016/j.bmcl.2018.12.012.

[13] *S. Cheng*, *Y. Zou*, *X. Chen*, *J. Chen*, *B. Wang*, *J. Tian*, *F. Ye*, *Y. Lu*, *H. Huang*, *Y. Lu*, *D. Zhang*, Design, synthesis and biological evaluation of 3-substituted-2-thioxothiazolidin-4-one (rhodanine) derivatives as antitubercular agents against Mycobacterium tuberculosis protein

tyrosine phosphatase B, European Journal of Medicinal Chemistry, Vol. **258**, 2023 DOI: https://doi.org/https://doi.org/10.1016/j.ejmech.2023.115571.

[14] *J. Sun*, *H. Zhong*, *K. Wang*, *N. Li*, *L. Chen*, Gains from no real PAINS: Where 'Fair Trial Strategy' stands in the development of multi-target ligands, Acta Pharmaceutica Sinica B, Vol. **11**, Iss. 11, 2021, DOI: https://doi.org/10.1016/j.apsb.2021.02.023.

[15] *M. Kratky*, *P. Sramel*, *P. Bodo, M. S. Prnova*, *L. Kovacikova*, *M. Majekova*, *J. Vinsova*, *M. Stefek*, Novel rhodanine based inhibitors of aldose reductase of non-acidic nature with p-hydroxybenzylidene functional group, European Journal of Medicinal Chemistry, Vol. **246**, 2023, DOI: https://doi.org/https://doi.org/10.1016/j.ejmech.2022.114922.

[16] *A.K.D. bin Ahmad Kamar*, *L. Ju Yin*, *C. Tze Liang*, *G. Tjin Fung*, *V.R. Avupati*, Rhodanine scaffold: A review of antidiabetic potential and structure–activity relationships (SAR), Medicine in Drug Discovery, Vol. **15**, 2022, DOI: https://doi.org/https://doi.org/10.1016/j.medidd.2022.100131.

[17] *H. Rai*, *R. Singh*, *P.S. Bharti*, *P. Kumar*, *S. Rai, T. Varma*, *B.S. Chauhan*, *A.S. Nilakhe*, *J. Debnath*, *R. Dhingra*, *V.N. Mishra*, *S. Gupta*, *S. Krishnamurthy*, *J. Yang*, *P. Garg*, *S. Srikrishna*, *S. Kumar*, *G. Modi*, Rhodanine composite fluorescence probes to detect pathological hallmarks in Alzheimer's disease models, Sensors and Actuators B: Chemical, Vol. **407**, 2024, DOI: https://doi.org/https://doi.org/10.1016/j.snb.2024.135364.

[18] *I.H. Hiba*, *J.K. Koh*, *C. W. Lai*, *S. M. Mousavi*, *I.A. Badruddin*, *M. Hussien*, *J.P. Wong*, Polyrhodanine-based nanomaterials for biomedical applications: A review, Heliyon, Vol. **10**, Iss. 7, 2024, DOI: https://doi.org/10.1016/j.heliyon.2024.e28902.

[19] *J. Lin*, *C. Jiang*, *Z. Liu*, *J. Zhao*, *L. Huo*, *E. Fan, P. Zhang*, *K. Deng*, Porous hollow carbon microspheres from poly(aniline-co-rhodanine) prepared in micellar template for high-performance supercapacitors, Journal of Energy Storage, Vol. **83**, 2024, DOI: https://doi.org/https://doi.org/10.1016/j.est.2024.110674.

[20] *E. Altunbaş*, *R. Solmaz*, *G. Kardaş,* Corrosion behaviour of polyrhodanine coated copper electrode in 0.1M H_2SO_4 solution, Materials Chemistry and Physics, Vol. **121**, Iss. 1-2, 2010, DOI: https://doi.org/https://doi.org/10.1016/j.matchemphys.2010.01.047.

[21] *R. Solmaz*, *E. Altunbaş Şahin*, *A. Döner*, *G. Kardaş*, The investigation of synergistic inhibition effect of rhodanine and iodide ion on the corrosion of copper in sulphuric acid solution, Corrosion Science, Vol. **53**, Iss. 10, 2011, DOI: https://doi.org/https://doi.org/10.1016/j.corsci.2011.05.067.

[22] *S.A. Umoren*, *M.M. Solomon*, Protective polymeric films for industrial substrates: A critical review on past and recent applications with conducting polymers and polymer composites/nanocomposites. Progress in Materials Science, Vol. **104**, 2019, DOI: https://doi.org/https://doi.org/10.1016/j.pmatsci.2019.04.002.

[23] *G. Wang*, *Y. Huang*, *X. Tang*, *J. Li*, *J. Dai*, *B. Liu*, *J. Zhang*, *J. Xiong*, A rhodanine modified poly-triarylamine dye function as a hole transport layer for inverted perovskite solar cells, Dyes and Pigments, Vol. **222**, 2024, DOI: https://doi.org/https://doi.org/10.1016/j.dyepig.2023.111843.

[24] *M. Fan*, *L. Duan*, *Y. Zhou*, *S. Wen*, *F. Li*, *D. Liu*, *M. Sun*, *R. Yang*, Rhodanine side-chained thiophene and indacenodithiophene copolymer for solar cell applications, Materials Today Energy, Vol. **5**, 2017, DOI: https://doi.org/https://doi.org/10.1016/j.mtener.2017.07.007.

[25] *O.T. Matica*, *C. Musina*, *A. G. Brotea*, *E. M. Ungureanu*, *M. Cristea*, *R. Isopescu*, *G. O. Buica*, *A.C. Razus*, Electrochemistry of Rhodanine Derivatives as Model for New Colorimetric and Electrochemical Azulene Sensors for the Detection of Heavy Metal Ions. Symmetry, Vol. **15**, Iss. 3, 2023, DOI: https://doi.org/10.3390/SYM15030752.

[26] *E.M. Ungureanu*, *M. Popescu*, *G. L. Tatu*, *L. Birzan*, *R. Isopescu*, *G. Stanciu, G. O. Buica*, Electrochemical comparison on new (Z)-5-(azulen-1-ylmethylene)-2-thioxo-thiazolidin-4-ones. Symmetry, Vol. **13**, Iss. 4, 2021, DOI: https://doi.org/10.3390/sym13040588.

[27] *G.L. Arnold*, *I.G. Lazar*, *G. O. Buica*, *E.M. Ungureanu*, *L. Birzan*, New azulene modified electrodes for heavy metal ions recognition, Bulgarian Chemical Communications, Vol. **49**, Special Issue C, 2017.

[28] *L. Birzan*, *M. Cristea*, *C. C. Draghici*, *V. Tecuceanu*, *M. Maganu*, *A. Hanganu*, *A.C. Razus*, *G.-O. Buica*, *E.M. Ungureanu*, Vinylazulenes chromophores: Synthesis and characterization, *Dyes and Pigments*, Vol. **131**, 2016, DOI: https://doi.org/https://doi.org/10.1016/j.dyepig.2016.02.033.

[29] *E. Cordoş, T. Frenţiu, A.-M. Rusu*, Analiza prin spectrometrie de absorbţie moleculară în ultraviolet-vizibil, Editura Institutului Naţional de Optoelectronică, București, 2001.

[30] *A.E. Harvey*, *D. L. Manning*, Spectrophotometric Methods of Establishing Empirical Formulas of Colored Complexes in Solution, Journal of the American Chemical Society, Vol. **72**, Iss. 10, 1950, DOI: https://doi.org/10.1021/ja01166a044.

[31] *J. Molland*, Inner Complex Salts of the 8-Hydroxyquinoline-5-sulfonic Acid, Journal of the American Chemical Society, Vol. **62**, Iss. 3, 1940, DOI: https://doi.org/10.1021/ja01860a024.

[32] *O.-T Matica.*, Electrochemical and spectral studies on organic ligands in view of heavy metal determination using chemically modified electrodes, National University of Science and Technology POLITEHNICA Bucharest, PhD THESIS, 2024.

[33] *E.-M. Ungureanu; M. Popescu (Apostoiu), M.; G.-L. Tatu (Arnold); L. Birzan; R. Isopescu; G. Stanciu; G.-O. Buica*, Electrochemical Comparison on New (Z)-5-(Azulen-1-Ylmethylene)-2-Thioxo-Thiazolidin-4-Ones, Symmetry, Vol. **13**, 2021, 588. https://doi.org/ 10.3390/sym13040588.